

## $\pi-p$ -ELASTIC SCATTERING IN THE ENERGY REGION 750-1450 MeV

*P. J. Duke, D. P. Jones, M. A. R. Kemp, P. G. Murphy,  
J. D. Prentice, J. J. Thresher*

Rutherford High Energy Laboratory, National Institute for Research in Nuclear Science,  
Chilton, Didcot, Berkshire, England  
(Presented by J. J. THRESHER)

Differential cross-sections for  $\pi^+p$  and  $\pi^-p$  elastic scattering have been measured at the different incident pion laboratory momenta (in MeV/c) (see Table).

A secondary pion beam was produced from a beryllium target in the vacuum chamber of the 8 GeV proton synchrotron, Nimrod. A conventional beam transport system was used to

focus the beam on a liquid hydrogen target. Interactions occurring in this target were detected by an array of scintillation counters (see Fig. 1). Elastic events were selected by requiring the correct angular relationship between the scattered pion and the recoil proton detected in coincidence. The eighteen counters to the right of the beam defined the solid angles for

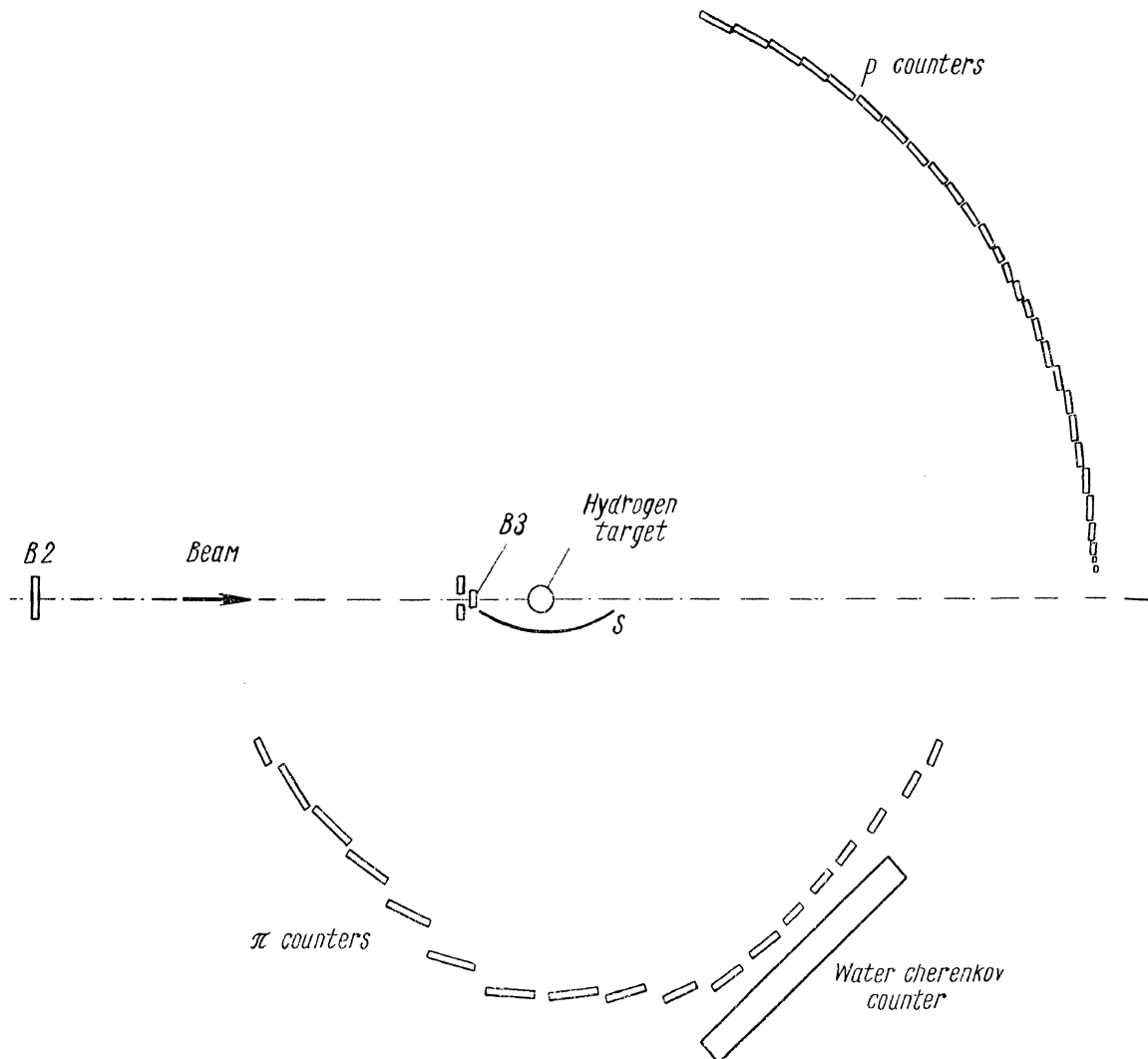


Fig. 1. Experimental layout.

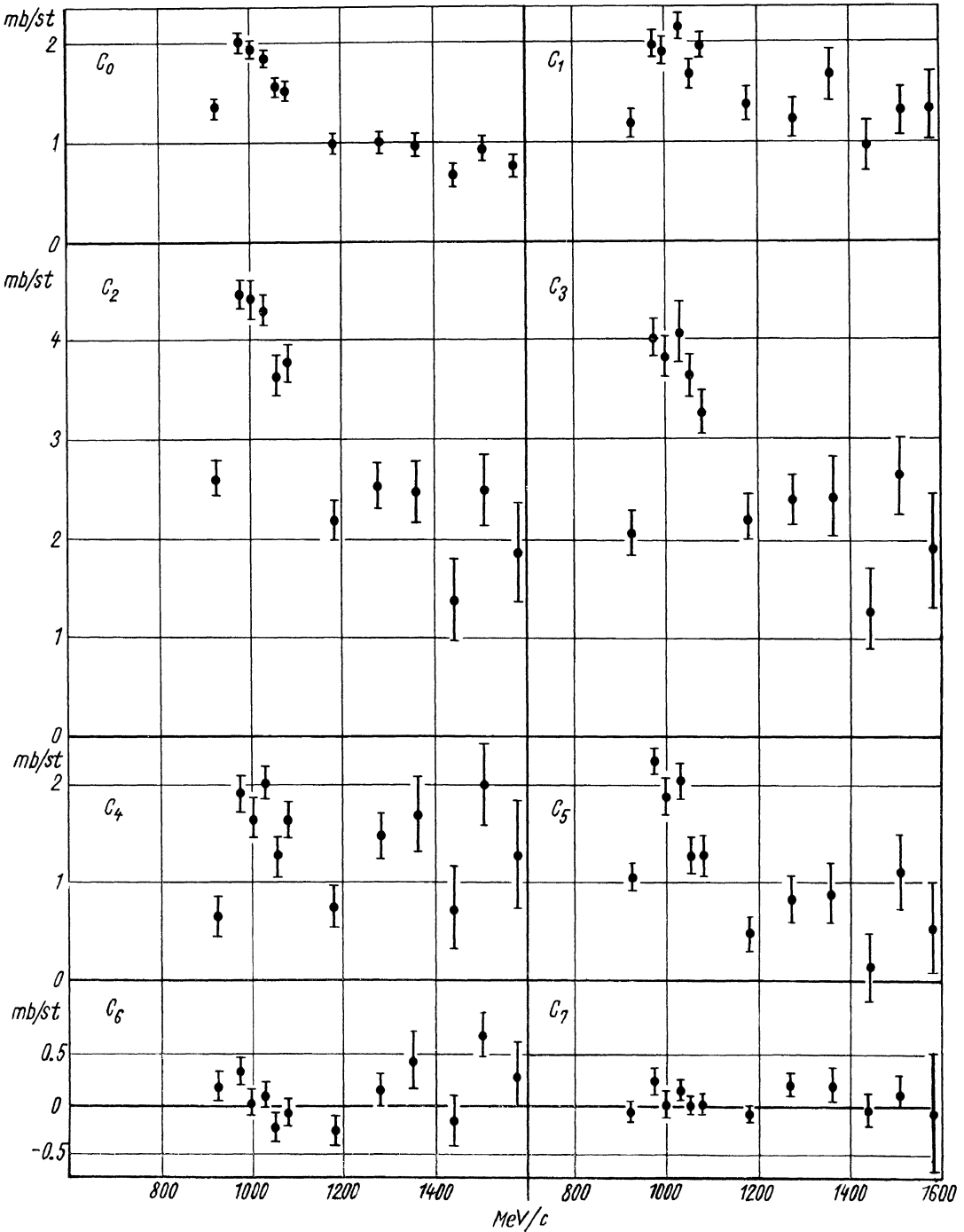


Fig. 2.  $\pi^-$ - $p$  elastic scattering  $\frac{d\sigma}{d\omega} = \sum C_l P_l(\cos \theta^*)$ .

detection of the scattered pions. In the energy region in question it was possible at most angles to discriminate between events in which a pion was scattered to the right of the beam, and events in which a proton was scattered to the right. In the range of laboratory angles from  $35^\circ$  to  $65^\circ$ , however, the angular correlation did

not resolve pions from protons. The ambiguity was resolved by requiring that the particle scattered to the right should also count in the water Cherenkov counter in coincidence with the relevant array counter.

After background subtraction, corrections were made for absorption of particles in the

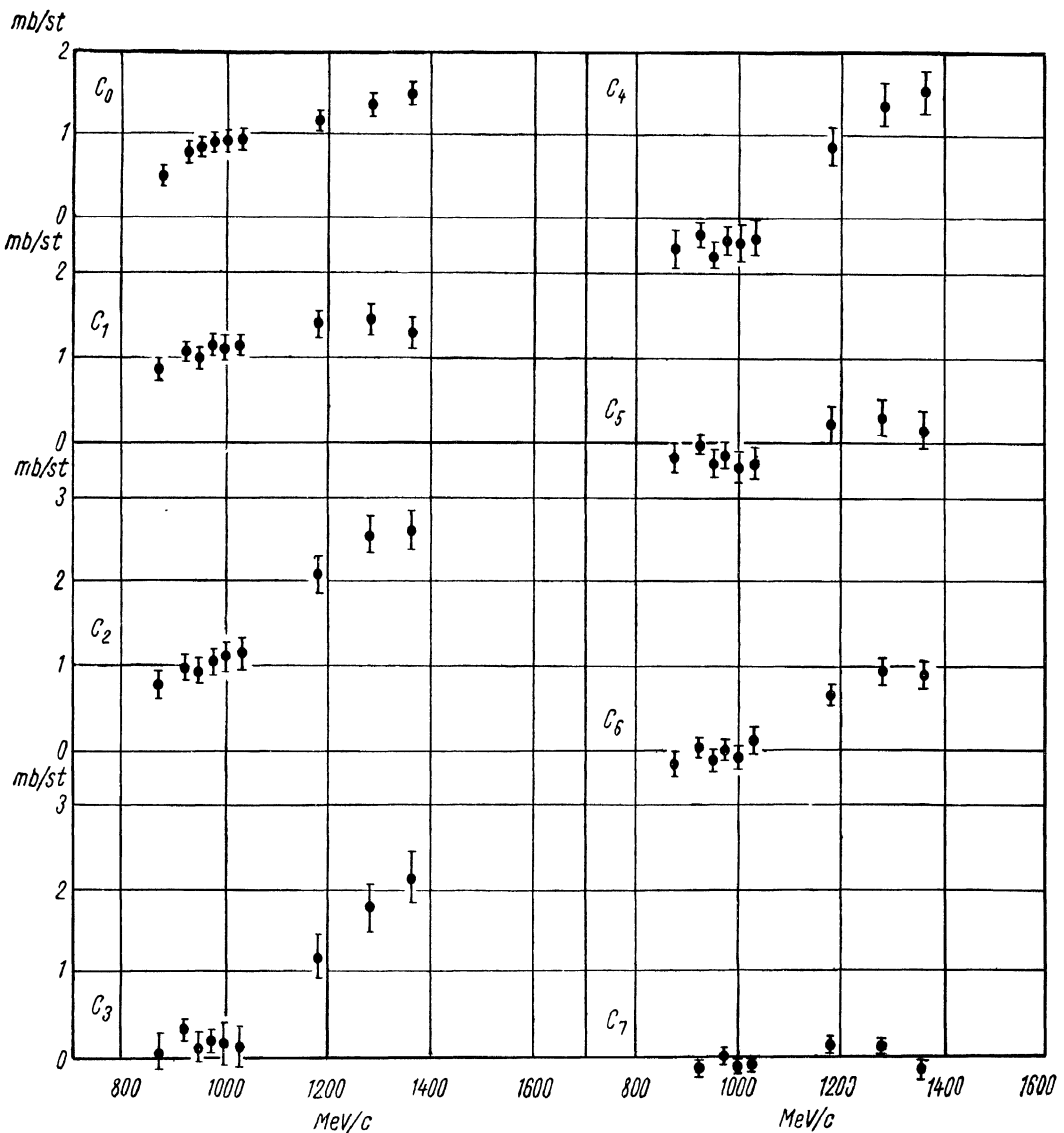


Fig. 3.  $\pi^+ - p$  elastic scattering  $\frac{d\sigma}{d\Omega} = \sum C_l P_l(\cos \theta^*)$ .

$\pi^-$	$\pi^+$	$\pi^-$	$\pi^+$
875	875	1080	1080
925	925	1180	1180
—	950	1280	1280
975	975	1360	1360
1000	1000	1440	—
1030	1030	1505	1505
1055	—	1579	1579

hydrogen target, muon and electron contamination of the beam and Cherenkov counter efficiency. A least squares fit was made to the resulting differential cross-sections in terms of Legendre polynomials:

$$\frac{d\sigma}{d\Omega} = \sum_l C_l P_l(\cos \theta^*)$$

The expansion coefficients  $C_l$  obtained from this analysis are shown below (see Fig. 2,3).

# CHARGE EXCHANGE AND $\eta$ PRODUCTION IN THE REGION BETWEEN THE SECOND AND THIRD $\pi-N$ RESONANCES

*A. Muller, E. Pauli, R. Barloutaud, J. Meyer*

Laboratoire de Physique Corpusculaire a Haute Energie, CEN-Saclay

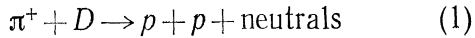
*M. Beneventano, G. Gialanella, L. Paoluzi*

Instituto di Fisica dell'Universita, Roma

Instituto Nazionale di Fisica Nucleare, Sezione di Roma

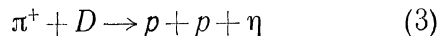
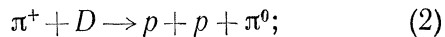
(Presented by A. LEVEQUE)

Using pictures from the 35 and 50 cm deuterium bubble chambers of Saclay, the reaction

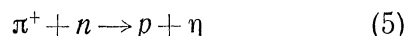
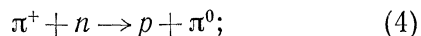


has been studied with incident pions of 600, 650, 750, 800, 850 Mev kinetic energies.

Kinematic fits for reactions



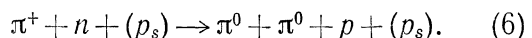
were applied to events which had two recognizable protons, one of which had a small momentum (1), in order to approximate the reactions



25% of the original sample were discarded as possibly non impulse model events.

The missing mass distribution is shown on Fig. 1, most events are clearly of type (2) or (3) where  $\eta$  decays through its neutral modes. The center of mass energy and production angle are calculated in the  $p\pi^0$  and  $p\eta$  systems for events in the two peaks of Fig. 1.

Impulse model events giving no fit for reactions (2) and (3) are considered examples of the reaction



Normalizing to the total neutral cross section  $\pi^- p \rightarrow \text{ neutrals}$  measured with counters (2) we obtain the cross-sections for reactions (4), (5) and (6) as a function of the c. m. energy as shown in Fig. 2. Contamination from reaction (6) in reaction (5) is evaluated at each energy and cross-section for  $\eta$  production is corrected for  $\eta$  charged decay mode.

The angular distribution of reaction (5) integrated over all energies (30% background events of reaction (6) are included) is shown to be compatible with isotropy.

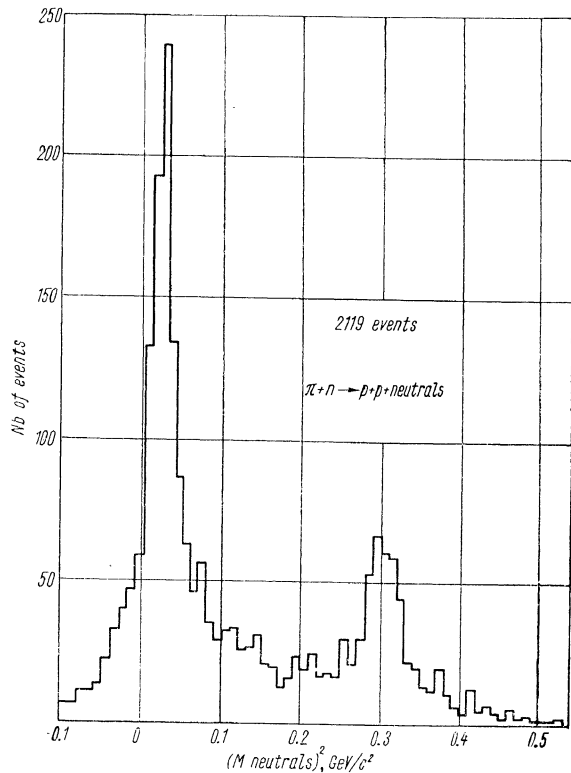


Fig. 1.

Differential cross-sections for reaction (4) and coefficients in the expansion  $\frac{d\sigma}{d\omega} = \sum a_n \cos^n \theta$  are given respectively in Fig. 3 and Table. The dominant effect is the rising of a backward bump at higher energies which is reflected by the large decrease of  $a_3$  and strong

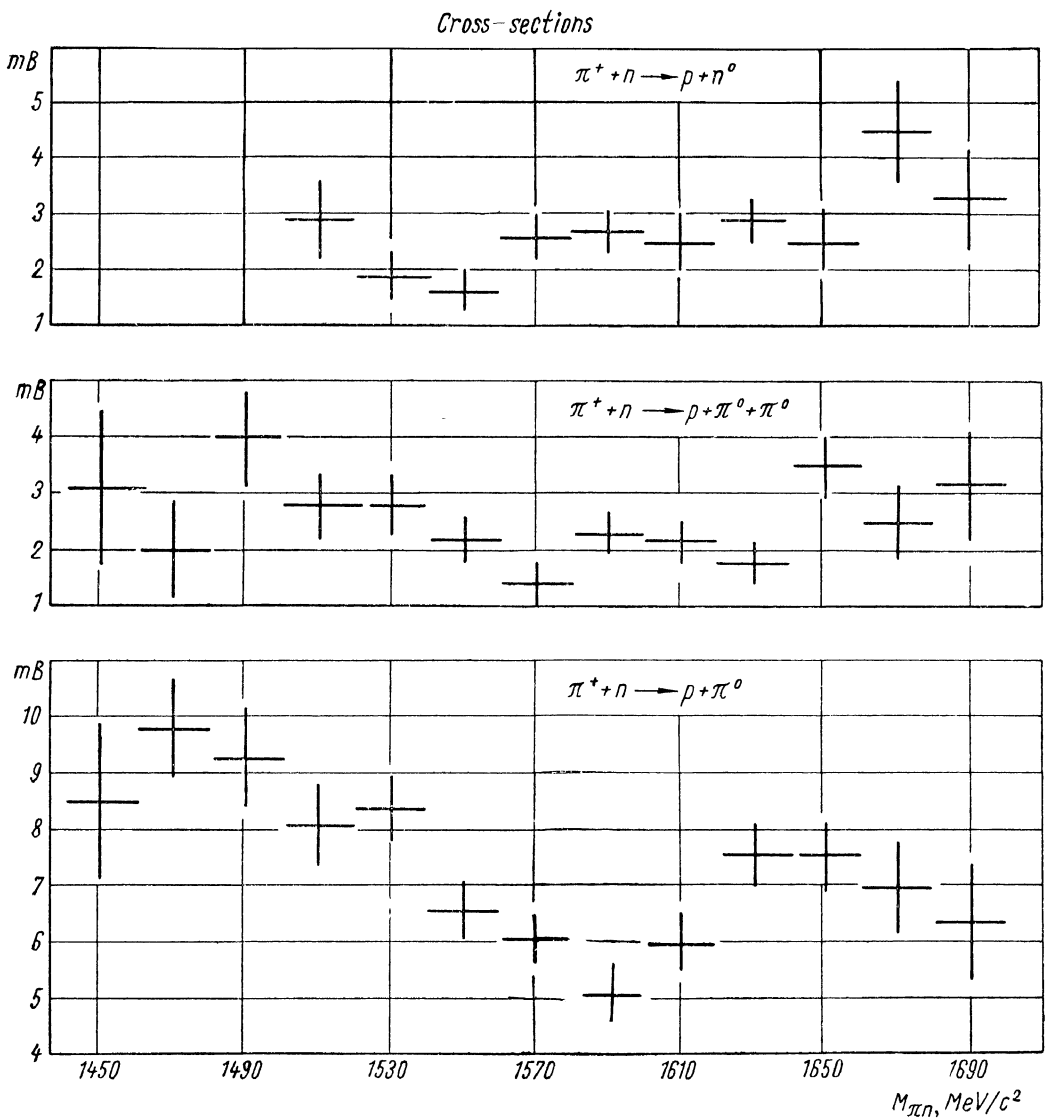


Fig. 2.

$E^*, \text{MeV}$	$a_0, \text{mb/ster}$	$a_1, \text{mb/ster}$	$a_2, \text{mb/ster}$	$a_3, \text{mb/ster}$	$a_4, \text{mb/ster}$	$a_5, \text{mb/ster}$	Total cross-section (mb)
1490–1530	$0,31 \pm 0,03$	$0,85 \pm 0,11$	$1,01 \pm 0,12$	$-0,15 \pm 0,24$	—	—	8,1
1530–1570	$0,23 \pm 0,06$	$0,21 \pm 0,19$	$0,89 \pm 0,23$	$0,65 \pm 0,36$	—	—	6,6
1570–1610	$0,12 \pm 0,03$	$0,15 \pm 0,19$	$1,08 \pm 0,36$	$-1,89 \pm 0,95$	$-0,31 \pm 0,55$	$2,47 \pm 1,05$	5,2
1610–1650	$0,16 \pm 0,03$	$0,34 \pm 0,15$	$0,38 \pm 0,31$	$-3,82 \pm 0,94$	$1,58 \pm 0,51$	$4,57 \pm 1,17$	7,6
1650–1690	$0,2 \pm 0,05$	$0,96 \pm 0,25$	$0,11 \pm 0,51$	$-6,43 \pm 1,25$	$1,66 \pm 0,8$	$7,34 \pm 1,41$	7,2

increase of  $a_5$ , which indicates a strong  $D_{15}F_{15}$  interference near the third resonance.

The similarity between charge exchange and elastic  $\pi^-p$  differential cross-section indicates that  $\pi^+p$  interaction is dominated by the  $T = 1/2$  state and that interferences between the 2 isospin states do not play a dominant role.

#### REFERENCES

1. Müller P. A. et al. Internal report LPCHE 64-10, 1964.
2. Brisson J. C. et al. Proceedings of the International Conference on Elementary Particles, Aix-en-Provence, 1, p. 45, 1961.

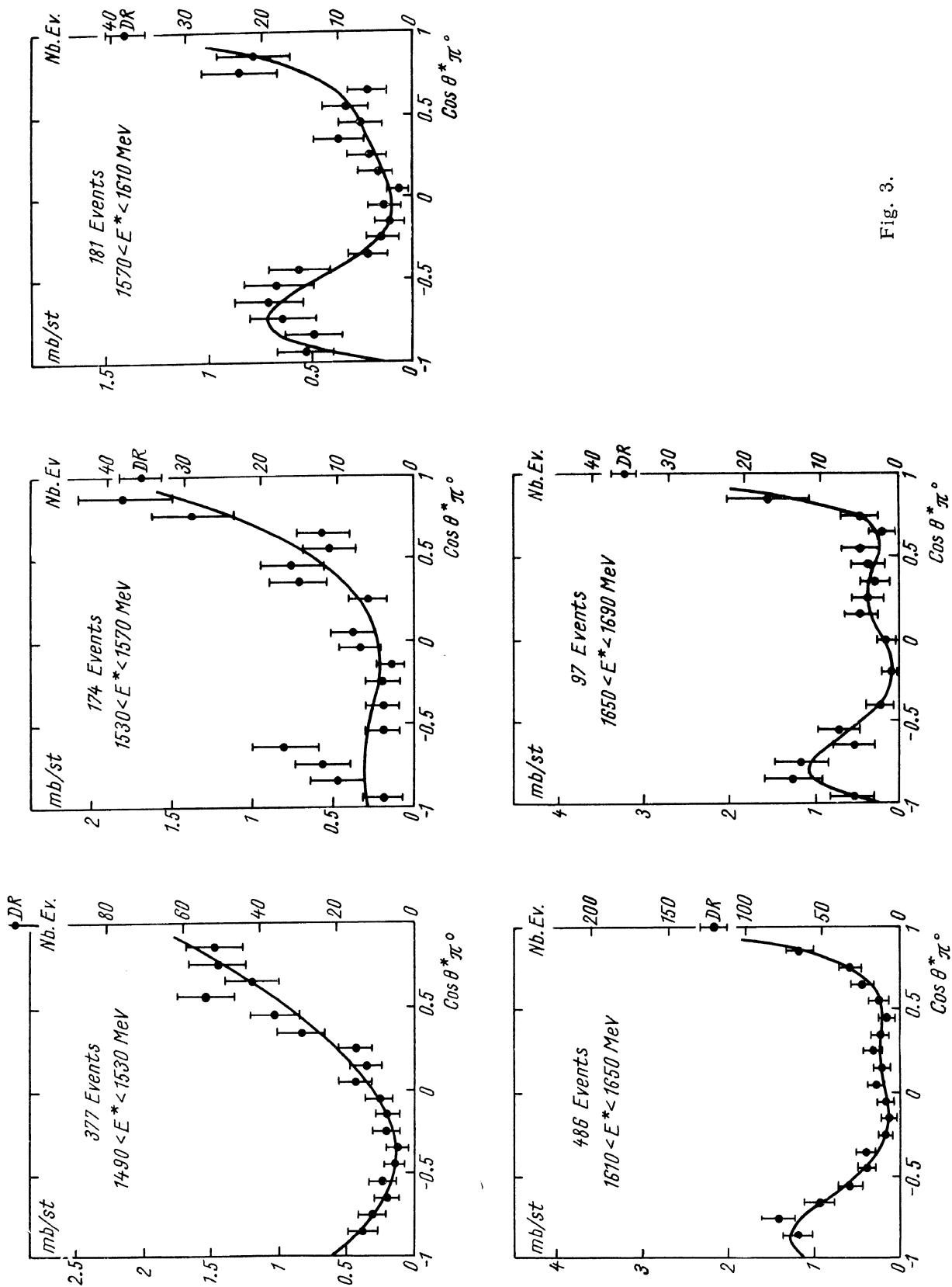


Fig. 3.